Egyptian Journal of Chemistry

http://ejchem.journals.ekb.eg/

Studies on the impact for pyrimidine compounds upon aluminium corrosion protection in acidic conditions, both experimentally and theoretically

Galal H. H. Ibrahim [a], Mohamed Abdelmotelb [a],Mohamed S. Elnouby [b] and M. A. Mostafa [a*]

[a] *Chemistry Department, Faculty of Science, Al-Azhar University, Assiut, 71524, Egypt*

[b] *City of Scientific Researches and Technology Applications , New Borg El Arab, Alexandria, Egypt*

Abstract

Using electrochemical, gravimetric, scanning electron microscopy and theoretical calculations, pyrimidine compounds are assessed for aluminum corrosion prevention in 1.0 M hydrochloric acid solution at various temperatures. According to the experimental procedures, all Pyrimidine compounds exhibit extremely good inhibitory efficiency when their concentration range (50-500 ppm) is increased at various temperatures. All of the studied inhibitors behaved as mixed type inhibitors, according to Tafel polarization curves. Based on the analysis of the relationship between temperature and corrosion inhibition, the thermodynamic and adsorption parameters were estimated and discussed. Aluminum surfaces were examined using scanning electron microscopy in both the absence and presence of inhibitors. Density functional theory was employed in theoretical calculations to forecast some parameters and the outcomes were generally in agreement the findings of experiments.

1. Introduction

Due to its superior mechanical attributes and low cost, aluminum (AL) is employed as a construction material and in machinery across a wide range of sectors, which has a significant economic and industrial significance [1, 2]. The use of natural products, organic, and inorganic chemicals in acidic conditions has been extensively explored to reduce AL corrosion. [3–10]. In order to stop the corrosion attack on metals, industrial acid cleaning, acid descaling, acid pickling, and oil well acidizing processes frequently use corrosion inhibitors for organic compounds containing oxygen, sulphur, nitrogen, and phosphorus atoms as well as functional groups like (-NH-, -N=N-, C=N, CHO, and R-OH [11–14]. The chemical structure of the compounds, the functional group, the charge surface of the metal, the quantity and charge density of adsorption sites, the molecular size, the heat of hydrogenation, the mode of interaction with the metal surface, and the formation of metallic complexes, all affect how effective an organic compound is at inhibiting a reaction. [15, 16]. Since many decades, pyrimidine compounds containing the functional -N=N- group have been used extensively in chemical synthesis [17, 18]. The effectiveness of pyrimidine derivatives to suppress corrosion of AL has been examined in numerous prior studies. But the purpose of our research, which is an expansion of our most recent publication [19]. In order to clarify the mechanism of corrosion inhibition of heterocyclic organic compounds, the molecular structure, the electronic structure, and the reactivity have been determined using the density functional theory (DFT) [20, 23].

We study the pyrimidine compound's ability to prevent aluminum corrosion in acidic solutions and associate this ability with the investigated compounds. quantum chemical properties are, E_{Homo}, E_{Lumo}, ΔE, μ, and parameters that provide important details about the reactive behaviour, such as TNC, η, σ, and ΔN., are among the estimated parameters.

2. Experimental details

2. 1. Materials

2. 1. 1. Inhibitors

Some pyrimidine derivatives as corrosion inhibitors that used throughout all the experiments were prepared by M. S. Tolba et al [24] and represented in (Table 1).

*Corresponding author e-mail: Ma.abdelhakeim@yahoo.com

Receive Date: 04 February 2023, **Revise Date:** 14 March 2023, **Accept Date:** 20 March 2023,
First Publish Date: 20 March 2023
DOI: 10.21608/EJCHEM.2023.190675.7559

2. 1. 2. Composition of Aluminum

The EGYPT ALUMINIUM COMPANY S.S.A.E (Qena), Nag Hammadi, Qena, Egypt, provided the aluminum samples utilised in the electrochemical tests. The samples were 1×5×0.2 cm3 in size and had an aluminum content of 99.98%. To prepare an aluminum working electrode for electrochemical measurements, specimens were polished with emery papers (1100–1600 grade) to create a smooth surface. This surface was then cleaned with distilled water, degreased with acetone for about some minutes, and then dried by filter papers at 30 ºC. [19]

2. 1. 3. Solutions.

HCl solutions was used to create the corrosive medium, which was then analytically processed to create a secondary standard solution with a concentration of 1.0 M and an average purity between 35 and 38 percent. The following percents of the standard HCl solution were used to prepare the inhibitor concentrations: 50, 100, 200, and 500 ppm.

2. 1. 4. Corrosion Cell

The corrosion cell utilised in this investigation had three electrodes: a counter (platinum wire electrode), a reference (saturated calomel electrode) and working electrode electrode (aluminium). One centimetre squared of the working electrode is exposed to solutions.

2. 2. Methods

2.2.1. Electrochemical Measurements

2.2.1.1. Open circuit potential (OCP)

Open circuit potential (OCP) is measured when the electrode is submerged for half an hour in the tested solutions at various temperatures in order to establish a steady state potential. OCP is a relationship between time (Min) vs potential (mV) at zero current (I=0) (Es.s).

2.2.1.2. Potentiodynamic polarization

Model 352/252 corrosion measurement system, which uses EG & G potentiostat/galvanostat model 273A operated by software from IBM computer, was used to measure OCP and polarisation curves [19, 25]. Linear polarisation resistance (LPR) was measured from +20 mV up to -20 mV vs. Ecorr and Tafel plot polarisations (TFP) were measured from -250 mV up to +250 mV vs. Ecorr. LPR and TFP measurements had scan rates of 0.166 mV/S and 0.3 mV/S, respectively. [19, 26]

From the following equations, the inhibitory effective ness (IE %) and surface coverage (θ) were computed (1, 2) [27]:.

$$\text{IE \%} = \left[\frac{(\text{C. R Free} - \text{C. R ihn})}{\text{C. R ihn}}\right] \qquad (1)$$

Where:

C.R. (Free) and C.R. (inh) are the corrosion rate without and with inhibitors, respectively.

$$\theta = \frac{\text{IE \%}}{100} \qquad (2)$$

2.2.1.2.1. Determination of the thermodynamic and activation parameters:

2.2.1.2.1.1. Activation energy (Ea)

Using the Arrhenius equation, the activation energies for AL corrosion in the presence and absence of inhibitors were determined. (3) [27]:

$$\log CR = \frac{-Ea}{2.303RT} + \log A \ldots\ldots (3)$$

Where:

Ea is the activation energy for the reaction

R is the molar gas constant is = 8.31 J mol^{-1} K^{-1}.

A is the Arrhenius pre-exponential factor.

The Arrhenius plot of log CR against 1/T gave straight lines with a slope of –Ea/2.303R for AL in the absence and presence of various concentrations of compounds P1 and P2 at temperatures 303, 313, 323 and 343K

2.2.1.2.1.2. Enthalpy of activation (ΔH^*) and entropy of activation (ΔS^*):

By the transition state equation, the values of the enthalpy of activation (ΔH^*) and entropy of activation (ΔS^*) of P1 and P2 chemicals on AL surface were computed. (4) [27]:

$$\text{CR} = \frac{\text{RT}}{\text{NAh}} \exp\left(\frac{\Delta S}{R}\right) \exp\left(\frac{\Delta H}{RT}\right) \ldots . (4)$$

Where:

h is Planck's constant.

N_A is Avogadro number.

A plot of log (CR/T) against 1/T gave straight lines with a slope of $-\Delta H^*/2.303R$ and an intercept of $[\log(R/N_A h) + (\Delta S^*/2.303R)]$ for AL in the absence and presence of P1, and P2 compounds contenting concentration (50 to 500) ppm in 1.0 M HCl solution at a temperature range of (303 to 343) K.

2.2.1.2.2. Determination of Adsorption Isotherms:

2.2.1.2.2.1. Adsorption Isotherms:

The obtained surface coverage was fitted in adsorption isotherms such the Langmuir adsorption isotherm, which many researchers have used to examine the adsorption process, in order to thoroughly investigate the mechanism of pyrimidine derivatives adsorption onto the aluminum/solution interface. Equation (5) gives the mathematical expression for the Langmuir adsorption isotherm [2, 6, 8, 19, and 27].

$$\frac{\theta}{1-\theta} = K\,C \ldots\ldots\ldots (5)$$

Where: K is the adsorption constant ($ml^{-1}L$), C is the concentration of the inhibitors. Rearranging the above equation (6)

$$\frac{C}{\theta} = \frac{1}{Kads.} + C \dots\dots\dots (6)$$

If the adsorption process follows the Langmuir adsorption isotherm, a straight line is produced between (C_{inh}/ θ) and C_{inh} values.

2.2.1.2.2.1.1. Gibbs Energy ΔG_{ads}:

The following equation connects the values of K_{ads} obtained from adsorption isotherms to ΔG_{ads} (7) [15, 20].

$\Delta G_{ads} = -RT \ln (1 \times 10^{6} K_{ads}) \dots\dots\dots (7)$

Where R: the constant of universal gas, 1×10^{6}: pure water concentration,

T: the absolute temperature.

2.2.1.2.2.1.2. Enthalpy (ΔH_{ads}) and Entropy (ΔS_{ads}):

Using the following equations, the enthalpy (ΔH_{ads}) and entropy (ΔS_{ads}) of adsorption are determined [23]:

$$\ln K ads = \frac{-\Delta Hads}{RT.} + constant \dots\dots\dots (8)$$

$\Delta G_{ads} = \Delta H_{ads} - T\Delta S_{ads}$ (9)

Adsorption can be physical, chemical, or of a mixed kind for exothermic processes (ΔH_{ads}<0), but it is related to chemisorption for endothermic processes (ΔH_{ads} > 0). Physisorption connected to (ΔH_{ads}) is roughly -40 kJ mol^{-1} or less negative for the exothermic process, whereas chemisorption related to "H ads" is roughly -100 kJ mol^{-1} or greater negative.

2.2.2. Gravimetric technique

The samples were polished with different emery sheets, cleaned in acetone, rinsed in distilled water, dried, and the constant weight (W1) was determined with an electronic balance. The test pieces were suspended using appropriate glass hooks in 100 mL of test solution in a 250 mL glass beaker that contained a certain quantity of each of four distinct chemical compounds. The specimens were removed from various aquatic environments after one day of immersion, cleaned with distilled water, dried, and again abraded with emery paper to remove the upper material and properly weighted (W2). W1-W2 is used to compute the WL. The inhibitor is present at concentrations of (50 to 500) ppm. The corrosion inhibition tests were carried out at 30 ºC. Based on the results obtained using Eq. (10), the corrosion rate (C.R.) in mm/year can be approximately calculated.

$$C.R. = \frac{K \times \Delta W}{A \times t \times d} \qquad (10)$$

Where K is a constant (8.76×10^{4}), A is the metal surface area (cm2); t is the immersion time (h), d is the metal density (g/cm3). The (IE_{WL}, %) and the (θ) of inhibitors were calculated using the following expression (11) [28].

$$IE_{WL}\% = \theta \times 100 = \frac{C.R._{.blank} - C.R._{.inh}}{C.R._{.blank}} \times 100 \qquad (11)$$

2.2.3. Scanning Electron Microscope (SEM)

One technique that explains the surface morphology of the uninhibited and inhibited AL samples is scanning electron microscopy (SEM). SEM photos were captured by the electron microscope unit of Assiut University in Assiut, Egypt (71526).

2.2.4. Quantum chemical calculations

DFT produced with GaussView 5.0 using the Gaussian 09W software using the 6-311G (d, p) basis set and Becke's three parameter exchange functional (B3LYP), quantum chemical computations of various parameters were performed [29, 30]. The equations (12-17) were used to calculate various quantum parameters, including the highest occupied molecular orbital (E_{HOMO}), the lowest unoccupied molecular orbital (E_{LUMO}), the energy gap (ΔE), the global hardness (η), the softness (σ),the dipole moment (μ), the total negative charges (T.N.C), the fraction of electrons transferred (ΔN) (12-17) [31–34]:

$\Delta E = E_{LUMO-HOMO}$ …… (12)

$A = -ELUMO \dots\dots\dots\dots (13)$

$I = -EHOMO \dots\dots\dots (14)$

$\eta = \frac{I-A}{2} \dots\dots\dots (15)$

$\sigma = \frac{1}{\eta} \dots\dots\dots (16)$

$$\Delta N = \frac{[\chi Fe - \chi inh]}{2[\eta Fe + \eta inh]} \dots (17)$$

Where $\chi_{Fe} \approx 7$ eV [29] is taken for iron and $\eta_{Fe} = 0$ is taken, assuming that the ionization potential, I, equal the electron affinity, A, for bulk metals where χ_{Fe} and η_{Fe} are 7 and 0 respectively [30].

3. Results and Discussions:

3.1. Electro Chemical Measurements

3.1.1. Open circuit potential measurements

Figure (2) illustrates how the (OCP) of AL changes over time in a solution of 0.1 M HCl in the presence and absence of various concentrations of (P1 and P2) compounds that act as inhibitors at a given temperature 30 ºC. In this instance, the OCP trend is similar; the OCP value first rises dramatically to more noble values before plateauing. This graph suggests that the corrosion process slows down with time until reaching steady-state rate within the time period shown. [31]. The plateau OCP value rises to more noble levels as the concentration of inhibitors in the electrolyte increases, demonstrating the adsorption of (P1 and P2) on the AL surface and its effect on the anodic corrosion reaction. [31,32 and 33].

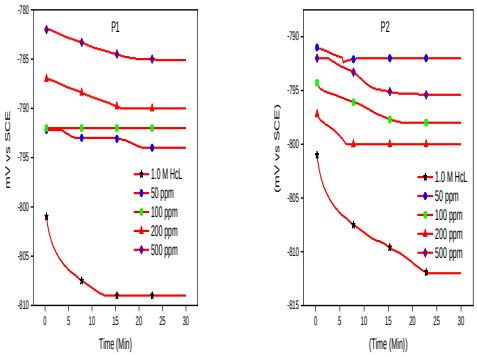

Figure1. Potential-time curves for aluminum in 1.0 hydrochloric acid solution at different concentrations of organic pyrimidine (P1and P2) compounds at 303

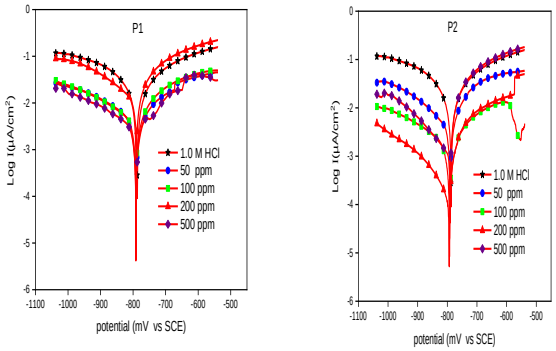

Figure 2. Tafel plot polarization curves of aluminum in hydrochloric acid solution at different concentrations of organic pyrimidine (P1and P2) compounds at 303K

3. 1. 2. Polarization Measurements:

A set of Tafel curves for the corrosion of aluminum in the without and wirh of (P1 and P2) compounds at concentrations of 50 to 500 ppm in 1.0 M HCl solution at 30 C are shown in Fig. (2). It is evident that as the concentration of (P1 and P2) in the bulk solution rises, the cathodic and anodic currents decrease, demonstrating the inhibitory impact of (P1 and P2) on corrosion. This shows that (P1 and P2) function as mixed-type corrosion inhibitors as well. The related inhibition efficiency, which was calculated using Eq. (12), and the accompanying corrosion current densities (icorr) are shown in (Table 2) together with the extrapolated cathodic and anodic curves to the relevant OCP. The data demonstrate that when the concentration of inhibitors in the bulk solution increases, the effectiveness of the corrosion inhibition likewise rises, reaching a maximum value of (P1= 91.69%) at room temperature, suggesting good surface corrosion protection by (P1 and P2) molecules. Additionally, (Table 2) calculated trend shows that the effectiveness of corrosion prevention is dependent on the surface concentration (coverage) of the P1 and P2 molecules that make up the protective layer . The gathered information unequivocally demonstrates that (P1 and P2) are very effective AL corrosion inhibitors at all the tested temperatures. This was an unexpected outcome because it was anticipated that (P1 and P2) would desorb at higher temperatures and provide less effective inhibition. However, it appears that the molecules on the AL surface are fairly stable over the entire temperature range investigated. This is a significant finding from a practical standpoint since it allows for the use of the inhibitor in more industrial processes that take place at somewhat higher temperatures. [34].

3. 1. 2. 1. Effect of Temperature:

The phenomenon of corrosion is significantly influenced by temperature. Corrosion occurs more quickly at higher temperatures. The majority of chemical and electrochemical reactions speed up as the temperature rises. [35-37]. We performed electro-measurements at temperatures equal to 303, 313, 323 and 343K to determine the impact of temperature on the behaviour of the inhibitors (P1 and P2) under study. The variations in the corrosion rate logarithm as a function of the reciprocal of the absolute temperature are shown in Figs. (3). Based on the findings in Table 3. The activation energy values in the presence of (P1 and P2) are higher than those that correspond to 1.0 M HCl alone, as can be seen. It is typical of physisorption inhibitors on the AL surface for Ea values to rise in the presence of inhibitors. [38-39]. These findings demonstrate that (P1 and P2) contribute to a stronger physical adsorption by producing a more surface, adhering, and thus more potent layer. [40-44]. In fact, 1.0 M HCl hydrochloric acid can be used to protonate pyrimidine heterocycles, which have many nitrogen atoms in their structure, to produce the ammonium action. It seems sense to infer that the quaternary cations adsorption electrostatics in this situation is what gives these compounds their excellent protective properties. Figure (4) displays the relationship between log (C.R./T) and 1000/T, which results in lines that are straight and have a slope of -ΔH/2.303R and an intercept of [log(R/NAh) + (ΔS/2.303R)] for AL in the absence and presence of P1 and P2 compounds at concentrations of (50 to 500) ppm in a 1 M HCl solution, respectively.

Table (2) Potentiodynamic parameters of some pyrimidine (P_1 and P_2) compounds on the corrosion of AL in 1.0

M HCl at 303 K.

Tested Solution	Conc. Ppm	R_P (Ω)	$ß_a$ mV\decade	$ß_c$ mV\decade	Ecorr- (mV)	Icorr (µA/Cm^2)	C.R (mpy)	η.p (%)	Surface coverage (θ)
HCl 1.0 M	-----	44.18	١٠١	156	٤٦٩	720	641.00	----	------
P 1	50	55.14	106	157	471	370	٣١٠	53.17	0.53
	100	69.54	111	201	455	320	٢٨٠	57.71	0.58
	200	80.14	147	211	454	255	٢٢٠	66.77	0.67
	500	83.01	125	214	451	75	٥٥	91.69	0.92
P 2	50	51.09	201	185	462	419	380	42.60	0.43
	100	57.23	211	201	451	395	355	46.38	0.46
	200	63.50	222	198	465	239	290	56.19	0.56
	500	74.25	232	145	466	139	101	84.74	0.85

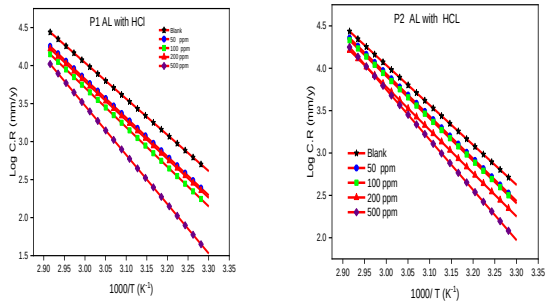

Figure 3. Arrhenius plots for AL in 1.0 M HCl solution at different pyrimidine concentrations.

Enthalpy readings that are positive show that the process of dissolving AL is endothermic. [45]. Further evidence from endothermic processes shows that AL dissolution is temperature-dependent, increasing with higher temperatures and decreasing at lower ones. Negative values of ΔS* indicate the development of activated complex in the rate-determining phase, which indicates association rather than dissociation. Accordingly, the disorder decreases as one moves from reactants to activated complex. [45, 46 and 47]. Additionally, data in (Table 3) show that Ea and ΔH* change in a similar way. The values of both Ea and ΔH* rise as inhibitor concentration rises, indicating that the energy barrier also rises. This implies that as the concentration of inhibitor increases, the corrosion reaction will be further driven to surface regions that are characterised by progressively higher values of Ea [45, 48, and 49].

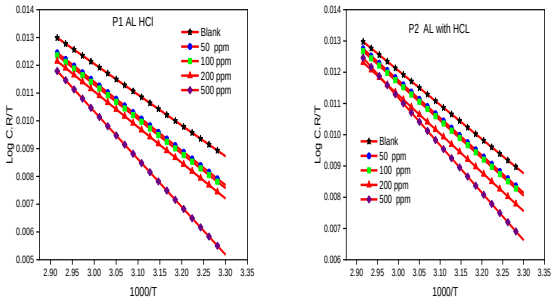

Figure 4. Transition state plot for AL in 1.0 M HCl at different concentration of pyrimidine concentration

Table (3) Thermodynamic parameters for the AL adsorption in blank solution without and with of some organic pyrimidine compounds at different temperatures

Tested Solution	Conc. ppm	E_a (kJmol^{-1})	ΔH* (kJmol^{-1})	Δs* (Jmolk^{-1})
HCl 1.0 M	------	-152.57	-89.15	-90.95
P 1	50	-168.31	-82.99	-97.54
	100	-167.63	-92.98	-97.56
	200	-172.35	-94.94	-99.63
	500	-240.89	-106.20	-123.99
P 2	50	-164.96	-87.47	-95.99
	100	-165.93	-87.81	-96.47
	200	-173.07	-96.02	-99.16
	500	-220.34	-114.97	-115.66

3. 1. 2. 2. Isotherms of Adsorption:

Fig. (5) demonstrates that at different temperatures, the variation of the ratio C/VS C ppm dependent on the inhibitor concentration is linear (303, 313, 323 and 343K). This shows that the Langmuir isotherm with a slope value equal to 1 governs the adsorption of (P1 and P2) on the surface of AL in 1M HCl. The appropriate isotherm was selected using the correlation coefficient. (Table. 4). As can be observed, all values of the slopes and the linear correlation coefficients (R2) are quite close to one. Figure (6) displays the linear relationship between ln K_{ads} and 1/T; the values of K_{ads} have also been obtained. The equation (7) links the standard free energy of adsorption (ΔG_{ads}) and the constant of adsorption $K_{ads.}$ The value of (ΔGads) derived from the latter is grouped in (Table 4). The acquired negative values of (ΔGads) show that the P1 and P2 are strongly and spontaneously adsorbed on the metal surface. Several researchers have also suggested that when (ΔGads) is greater than -20 kJ/mol, this energy corresponds to the interactions between charged molecules and metal charges (physisorption), whereas when (ΔGads) is lower than -40 kJ/mol, it corresponds to a charge transfer between the inhibitor molecules and the metal surface by forming coordination bonds. [50, 51]. In our situation, we can see that the free enthalpy of adsorption values range from approximately -25.99 kJ/mol to -22.66 kJ/mol at various temperatures. This reveals that (P1 and P2) are firmly adsorbed on the surface of metal through chemical-adsorption with a propensity for physisorption, which involves an electron transfer between the nitrogen, sulphur, and aluminum atoms [52]. Examining the impact of heat on the inhibitory power reveals the possibility of the second mode (physical adsorption). The electrostatic interactions between (P1 and P2) charge's molecules and the charged metal are, in fact, what cause (P1 and P2) inhibitor's effects (physical-adsorption). This finding is confirmed by the observation that this compound's inhibitory potency noticeably declines at high temperatures. [53].

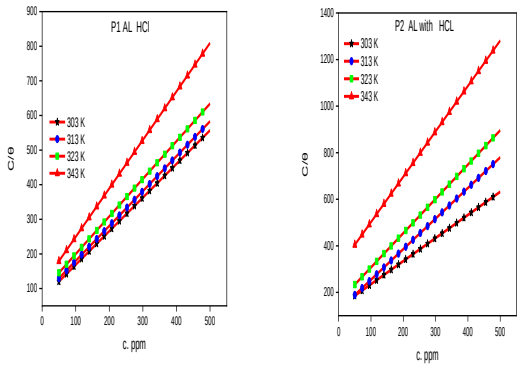

Figure 5. Curves fitting of some organic pyrimidine (P1and P2) compounds adsorption by Langmuir isotherm for aluminum in 1.0 M hydrochloric acid solution at different Temperatures.

Therefore, it may be stated that both chemisorption and physical adsorption are viable adsorption modalities. [54-56]. promoting the metals adsorption on the negative sites (physisorption) in the HCl medium.

The positive values of ΔH_{ads} demonstrated in Table 4 imply that the process of the inhibitors' adsorption is endothermic [55], and that the efficiency of the inhibition increases as the temperature rises. This behavior can be explained by the theory that the temperature increase caused inhibitor molecules to bind to the metal's surface.. As was predicted given that the endothermic adsorption process is usually accompanied by an increase in entropy, the values of Sads shown in (Table 4) have a positive sign. The catalyst for the adsorption of the inhibitor onto the AL surface was this increase in entropy [56, 57].

Table (4) Values of Langmiur adsorption parameters for adsorption the some organic pyrimidine compounds on the corrosion of AL in 1.0 M HCl at different temperatures.

Test solution	T (K)	R^2	$LogK_{ads}$	ΔG_{ads}. kjmol^{-1}	ΔH_{ads} (KJ/mol)	ΔS_{ads} (J/mol/K)
P 1	303 K	0.99	0.01497	-24.02	1.58	٧٩,٢٨
	313 K	0.99	0.01265	-23.74		٧٨,٣٤
	323 K	0.99	0.01047	-23.23		٧٦,٦٦
	343 K	0.99	0.00815	-22.67		٧٤,٤٧
P 2	303 K	0.99	0.01095	-24.97	2.026	٧٧,٢٩
	313 K	0.99	0.00894	-24.42		٧٥,٦١
	323 K	0.99	0.00867	-24.34		٧٥,٣٥
	343 K	0.99	0.00624	-23.46		٧٢,٦٢

3. 2. Gravimetric study

Through using weight loss method, the corrosion rate of AL at 30 oC in the absence and presence of various concentrations of (P1 and P2) was investigated. (Table 5) displays the calculated corrosion rate (mg cm-2 h-1), weight difference, and inhibition efficiency (IE_{WL}) for AL in 1.0 M HCl in the absence and presence of (P1 and P2), demonstrating the inhibitor's capacity to prevent corrosion of AL in 1.0 M HCl solution, where the corrosion rate is concentration-dependent. The effectiveness of the inhibition increases with concentration. Additionally, as displayed in Fig. 7, the results revealed that the corrosion rate decreased with concentration and that (P1 and P2) actually slowed AL corrosion in 1.0 M HCl.

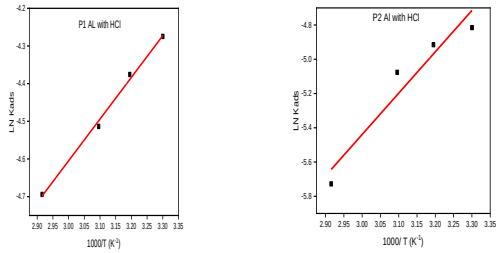

Figure 6. plot of ln K_{ads} against 1/T for AL in 1.0 M HCl solution at different pyrimidine compounds

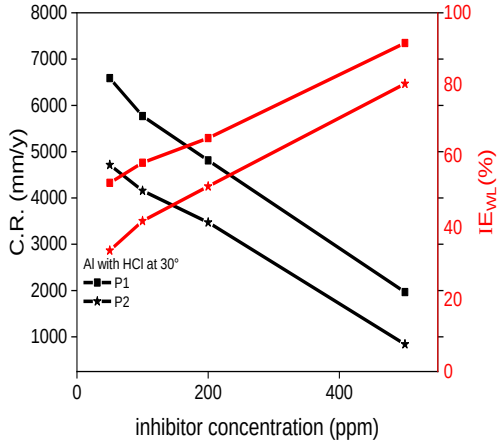

Figure 7. Relation between inhibitors concentration and C.R

3. 3. Scanning Electron Microscope Analysis

The morphology of the polished AL electrode surfaces before exposure to the corrosive medium is shown in Fig. 8A. After being submerged in 1.0 M HCl solution for 24 hours at room temperature, the surfaces of the AL electrode specimen under study are depicted in SEM image in Fig. 8B. The micrograph shows that there was significant surface damage. The corroded regions are depicted in the specimens as black grooves with grey and white zones that resemble the dandruff of aluminum oxides. The highly oxidized phase may have generated in air during desiccation with no surface protection. After being submerged for the same amount of time and at the same temperature in a solution of 1.0 M HCl containing 500 ppm, the surface of another AL electrode specimen is shown in SEM pictures in Fig. 8C. (p1). The micrograph shows that the metal surface has an excellent protective film and is smoother than the surface that is not inhibited. This attests to the inhibitor's greatest level of inhibitory effectiveness (p1).

Table (5). Weight loss parameters of P1 and P2 compounds as inhibitors on the corrosion of AL in 1.0 M HCl for 1 day.

Conc. Of inhibitors (ppm)	ΔW (g)	C.R (mm/y)	I.E_{WL} (%)
Blank	0.05132	9942.5690	.....
P1			
50	0.02433	4713.6146	52.5916
100	0.02145	4155.6529	58.2034
200	0.01792	3471.7622	65.0818
500	0.00433	838.8800	91.5627
P2			
50	0.02855	5531.1837	44.3687
100	0.02659	5151.4597	48.1878
200	0.02223	4306.7675	56.6836
500	0.00843	1633.2006	83.5737

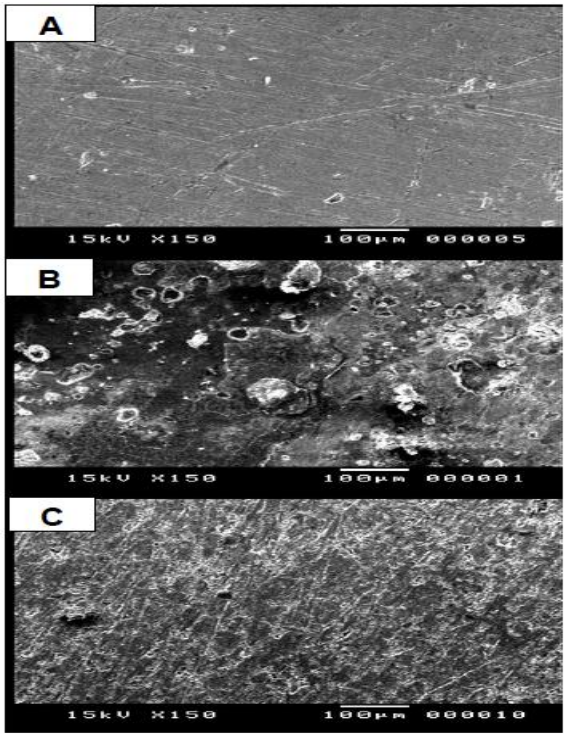

3. 4. Quantum chemical calculations

A number of adsorption centers, the mode of interaction with the surface of the metal, the size, and

the molecular structure are just a few of the variables that affect how organic compounds prevent metals from corroding in an acidic medium [58]. Additionally, in order to provide additional interpretations for the experimental data, various quantum parameters, such as E_{HOMO}, E_{LUMO}, $\Delta E = E_{HOMO} - E_{LUMO}$, (σ), (η), (μ, Debye) and (ΔN).

Table (6). The calculated theoretical chemical parameters of some organic pyrimidine (P1 and P2) compounds using (DFT) 6-311G (d, p) basis set method.

Method	DFT/B3LYP/6-311 G (d,p) Parameters								
Comp.	E_{HOMO} (ev)	E_{LUMO} (ev)	EΔ (ev)	η (ev)	σ (ev)	μ (Debye)	NΔ (ev)	T.N.C	$(\eta.p)^{*}_{Exp}$ %
P 1	-7.6743	-5.9867	1.6876	0.8438	1.1851	8.2404	0.1004	-5.703	78.31
P 2	-7.6776	-5.8487	1.8289	0.9144	1.0936	3.5274	0.1295	-5.281	68.83

*Average η.p values for different concentrations at room temperature

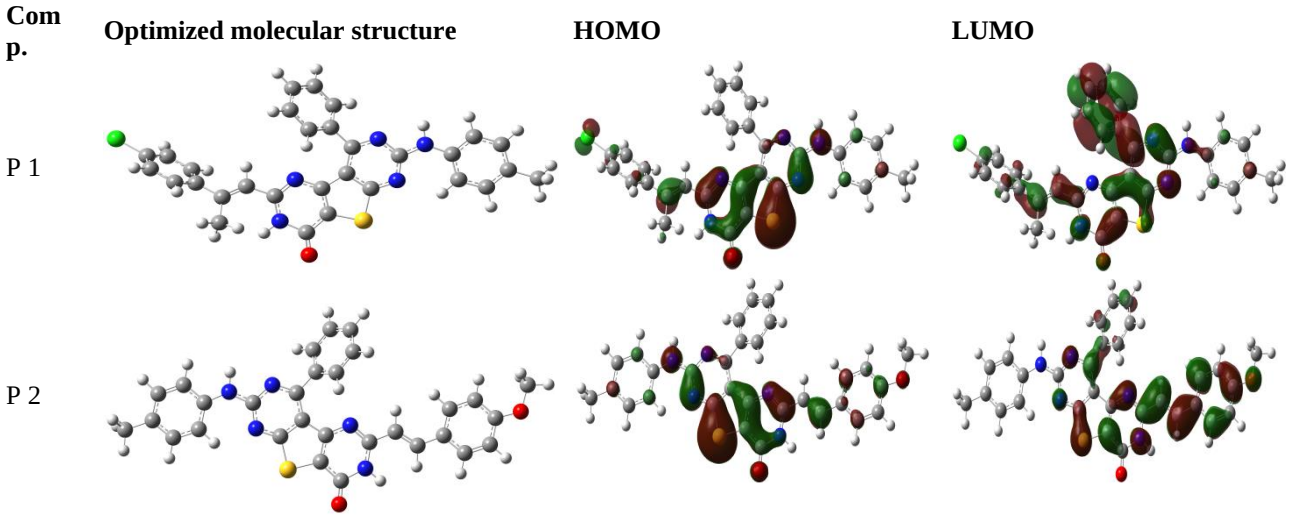

Figure 9. The Optimized molecular structure, HOMO and LUMO of the investigated (P1 and P2) using (DFT) 6-311G (d, p) basis set method.

According to its definition, E_{HOMO} (the energy of the first unoccupied molecular orbital) is frequently linked to a molecule's capacity to accept electrons. A high HOMO energy value encourages a molecule's propensity to donate electrons to species that receive them and have vacant molecular orbitals with low level energies. The ability of the molecule to take electrons is instead shown by E_{LUMO} (the energy of the highest occupied molecular orbital). If the ELUMO value is low, the molecule unquestionably receives electrons. The minimal energy needed to excite an electron in a structure is $\Delta E = E_{HOMO} - E_{LUMO}$. The result is a strong inhibitory efficacy at low values of ΔE [60-63].

(Table 6). Gather the P1 and P2 compounds' estimated quantum properties. These compounds can readily transfer one or more electrons from the HOMO level to the open "d" orbitals of iron, favoring the sharing of electrons between these molecules and the surface of the metal. As can be seen from Table (6), the molecules with lower energy gaps are those with better inhibitory efficiency. [64, 65]. However, research shows that a rise in E_{HOMO} values can speed up the process of adsorption by affecting how species are transported across the adsorbed layer [64]. It was evident from (Table 6) that the outcomes show that P1 is more efficient than P2 [66, 67].

A high absolute hardness value for a molecule is a sign of its great stability and minimal reactivity. [68]. It was evident from (Table 6) that for the examined inhibitors, the IE % values fall as the hardness values increase. The hardness substance is the inhibitor P2 (η =0. 9144). The hardness substance is the inhibitor P1 (η =0.8438). The increasing hardness values and the experimental IE % values agree well.

According to the type and nature of the molecules used, the inhibitory effectiveness rises as the dipole moment value does [69]. The values of. IE %
grew with rising values, as shown in (Table 6).The in

hibitor with the highest μ value is P1 (8.2404 D). The lowest μ value is for the inhibitor P2 (3.5274 D).

Thus according Lukovits' research, the ability of the inhibitor to donate electrons to the metal surface increases if the value of ΔN is more than 3.6. [70-72]. As per (Table 6), values of ΔN typically vary from 0.1004 to 0.1295. T1 denotes the highest electron transport and thus a higher IE%. Thus, when compared to the other inhibitor P2, P1 has the highest fraction of transmitted electrons.

By Mullikan population analysis is typically used to calculate the charge distribution throughout the entire skeleton of the molecules and to determine the adsorption centres of inhibitors [73, 74]. Select atoms of carbon, oxygen, and nitrogen had their computed Mulliken charges (total negative charges) shown in (Table 6). It is predicted that P1 will interact with the metal surface more frequently while P2 would do so less frequently.

Figure (9) shows how the molecules' HOMO and LUMO electron densities are distributed Thus; we see that the heteroatoms (S, N) of the pyrimido ring and pyrimidine are where the distribution of the HOMO density is centred for all inhibitory compounds. The existence of aromatic substituents with "" electrons, which encourage the sharing of electrons between these compounds and the metal surface, can be used to explain why pyrimidine has such a strong inhibitory potency. The concentration of anions (Cl^-) on the metal surface will also encourage the adsorption of the cationic versions of the pyrimidine inhibitors [75].The sulphur atom's immediate surroundings had the highest HOMO density values, which is conclusive proof that sulphur is the nucleophilic core [76, 77]. As a result, sulphur will easily form the connection with the metal, as opposed to N or C atoms..

4. Conclusions

The study of the inhibitory effect of a pyrimidine compounds derivatives, namely P1, P2, P3 and P4 against corrosion of aluminum in 1.0 M HCl medium allowed us to confirm its performance and draw the following conclusions:

- P1, P2, P3 and P4 of corrosion inhibition for aluminum in 1.0 M HCl, even at low concentrations.
- The inhibitory effect of P1, P2, P3 and P4 increases with increasing inhibitor concentration.
- The increase in temperature affects the inhibitory efficiency. In hydrochloric medium, the thermodynamic data obtained show a double aspect of adsorption (physisoprtion) of the P1, P2, P3 and P4 on the metals surface. In fact, the energy apparent activation of corrosion which is higher in the presence of P1, P2, P3 and P4 than in its absence, and the highest values of the free energy of adsorption verify the character physisorption of the most predominant adsorption.
- The inhibition is due to the adsorption of the inhibiting molecules on the surface of the steel and the blocking of its active sites.
- The adsorption of P1, P2, P3 and P4 follows the Langmuir adsorption isotherm.
- The molecules are adsorbed with the heteroatoms forming donor-acceptor bonds of unpaired electrons between heteroatoms and active centers on the metal surface. In decreasing the rate of corrosion.
- Quantum chemical calculation descriptors and calculated Mulliken charges showed that the priority of charge reallocation form inhibitor otal the negative charges to the metals surface is easier in the order: P1 > P2 > P3 > P4 which reveal good agreement to the electrochemical measurements. Based on DFT results, an inhibition mechanism was proposed.

5. Acknowledgments

Authors contributions to the manuscript
Galal H.H. Ibrahim and Mohamed Abdelmotelb carried out electrochemical measurements including potentiodynamic polarization, scanning electron microscopy (SEM) and temperature dependance measurements. M. S. Tolba synthesized the investigated inhibitors. M. A. Mostafa edited the electrochemical discussion for the re- vised manuscript and its corresponding replies to the referees. Mohamed S. Elnouby carried out the computations including DFT and adsorption annealing simulations and wrote the manuscript.

Declaration of Competing Interest

The authors declare that they have no known competing finan- cial interests or personal relationships that could have appeared to influence the work reported in this paper.

6. Reference

[1] S. Safak , B. Duran, A. Yurt and G. Türkog "Schiff bases as corrosion inhibitor for aluminium in HCl solution" Corrosion Science Volume 54, January 2012, Pages 251-259

[2] D. Brough and H. Jouhara "The aluminium industry: A review on state-of-the-art technologies, environmental impacts and possibilities for waste heat recovery" International Journal of Thermofluids 1-2 (2020) 100007

[3] T. Chen, H. Gan, Z. Chen,M. Chen and C. Fu "Eco-friendly approach to corrosion inhibition of AA5083 aluminum alloy in HCl solution by the expired Vitamin B1 drugs", J. of Molecular Structure, 1244 (2021) 30881—30894.

[4] N. Nnaji, N. a Nwaji, J Mack and T.

Nyokong " Corrosion resistance of aluminum against acid activation: impact of benzothiazole-substituted gallium phthalocyanine", Molecules 24 (2019)207-229.

[5] M. Husaini "Corrosion inhibition effect of benzaldehyde (Methoxybenzene) for Aluminium in sulphuric acid solution", Algerian J. of Eng. and Technology, 4 (2021) 074–080.

[6] N. S. Abdelshafi, M. A. Sadik, M. A. Shoeib and S. Abdel Halim "Corrosion inhibition of aluminum in 1 M HCl by novel pyrimidine derivatives, EFM measurements, DFT calculations and MD simulation", Arabian J. of Chemistry, 15(2022) 103459-103469.

[7] M. Husaini "Organic compound as inhibitor for corrosion of aluminum in sulphuric acid solution ",Algerian J. of Chemical Eng., 1 (2020) 22–30.

[8] M. Husaini, "Effect of Anisaldehyde as Corrosion Inhibitor for Aluminium in Sulphuric Acid Solution", J. of Science and Technology, 2 (2020) 1-10.

[9] M. A. Mostafa , A. M. Ashmawy , M. A.M. Abdel Reheim , M. A. Bedair , A. M. Abuelela "Molecular structure aspects and molecular reactivity of some triazole derivatives for corrosion inhibition of aluminum in 1 M HCl solution", J. of Molecular Structure, 1236 (2021) 130292–13310

[10] T. Zhang, W. Jiang, H. Wang and S. Zhang "Synthesis and localized inhibition behaviour of new triazine-methionine corrosion inhibitor in 1 M HCl for 2024-T3 aluminium alloy", Materials Chemistry and Physics, 237 (2019) 121866-121876.

[11] F. Bentiss, M. Lagrenée, M. Traisnel, C. Hornez, Corros. Sci. 1999, 41, 789.

[12] W.W. Frenier, F.B. Growcock, in: A. Raman, P. Labine (Eds.), Review on Corros. Sci. And Technology, NACE Int., Houston, TX. 1993, 11.

[13] F. Zucchi, G. Trabanelli, G. Brunoro, Corros. Sci. 1994, 36, 1683.

[14] B. Mernari, H. Elattari, M. Traisnel, F. Bentiss, M. Lagrenee, Corros. Sci. 1998, 40, 391.

[15] S. S. Mahmoud, Journal of Materials Sci. 2007, 42, 989.

[16] G. Gao and C. Liang. Jour. Of the Electrochemical Society (2007, 2, 144.

[17] Esvet Akbas, Ela Yildiz and Ahmet Erdogan " Synthesis, characterization and theoretical studies of novel pyrimidine derivatives as potential corrosion inhibitors" J. Serb. Chem. Soc. 85 (4) 481–492 (2020)

[18] K. Rasheeda, Vijaya D.P. Alva, P.A. Krishnaprasad and S. Samshuddin "Pyrimidine derivatives as potential corrosion inhibitors for steel
d medium – An overview" Int. J. Corros. Scale Inhib., 2018, 7, no. 1, 48 – 61

[19] M.A. Mostafa , Ashraf M. Ashmawy , M A.M. Abdel Reheim , Mahmoud A. Bedair and Ahmed M. Abuelela " Molecular structure aspects and molecular reactivity of some triazole derivatives for corrosion inhibition of aluminum in 1 M HCl solution" J. of Molecular Structure 1236 (2021) 130292.

[20] P. Senet, Chem. Phys. Lett. 1997, 275, 527.

[21] M.K. Awad , M.S. Metwally , S.A. Soliman , A.A. El-Zomrawy and M.A. bedair,"Experimental and quantum chemical studies of the effect of poly ethylene glycol as corrosion inhibitors of aluminum surface", Journal of Industrial and Engineering Chemistry 20 (2014) 796-808.

[22] S. Bashir, A. Thakur, H. Lgaz, I.Chung, and A. Kumar, "Corrosion inhibition efficiency of bronopol on aluminium in 0.5 M HCl solution: Insights from experimental and quantum chemical studies" Surfaces and Interfaces, 20 (2020)100542- 100553.

[23] N.S. Abdelshafi , M.A. Sadik, Madiha A. Shoeib and Shimaa Abdel Halim "Corrosion inhibition of aluminum in 1 M HCl by novel pyrimidine derivatives, EFM measurements, DFT calculations and MD simulation" Arabian Journal of Chemistry (2022) 15, 103459

[24] M. S. Tolba, A. M. Kamal El-Dean, M. Ahmed and R. Hassanien "Synthesis, reactions, and biological study of some new thienopyrimidine derivatives as antimicrobial and anti-inflammatory agents", J. Chin Chem Soc., 66 (2018) 1–10

[25] M.H. Mahross, M.A. Taher and M.A. Mostafa, International Journal of Adv. In Pharmacy, Biology and Chem. 2015, 14, 852.

[26] M.H. Mahross, M.A. Taher and M.A. Mostafa, Elixir Corros. 2015, 86, 34962.

[27] M. Shams El-Din and N. J. Panl, Desalination. 1988, 69, 251.

[28] M. Yadav, S. Kumar, I. Bahadur, D. Ramjugernath "Corrosion Inhibitive Effect of Synthesized Thiourea Derivatives on Mild Steel in a 15% HCl Solution", Int. J. Electrochem. Sci., 9(2014) 6529–6550.

[29] S. G. Zhang, W. Lei, .M. Z. Xia and F. Y. Wang, Jour. Of Molecular Strut. Theochem 2005, 732, 173.

[30] Gaussian 09, Revision A.02, M. J. Frisch, G.

W. Trucks, H. B. Schlegel, G. E. Scuseria, M. A. Robb, J. R. Cheeseman, G. Scalmani, V. Barone, B. Mennucci, G. A. Petersson, H. Nakatsuji, M. Caricato, X. Li, H. P. Hratchian, A. F. Izmaylov, J. Bloino, G. Zheng, J. L. Sonnenberg, M. Hada, M. Ehara, K. Toyota, R. Fukuda, J. Hasegawa, M. Ishida, T. Nakajima, Y. Honda, O. Kitao, H. Nakai, T. Vreven, J. A. Montgomery, Jr., J. E. Peralta, F. Ogliaro, M. Bearpark, J. J. Heyd, E. Brothers, K. N. Kudin, V. N. Staroverov, R. Kobayashi, J. Normand, K. Raghavachari, A. Rendell, J. C. Burant, S. S. Iyengar, J. Tomasi, M. Cossi, N. Rega, J. M. Millam, M. Klene, J. E. Knox, J. B. Cross, V. Bakken, C. Adamo, J. Jaramillo, R. Gomperts, R. E. Stratmann, O. Yazyev, A. J. Austin, R. Cammi, C. Pomelli, J. W. Ochterski, R. L. Martin, K. Morokuma, V. G. Zakrzewski, G. A. Voth, P. Salvador, J. J. Dannenberg, S. Dapprich, A. D. Daniels, O. Farkas, J. B. Foresman, J. V. Ortiz, J. Cioslowski, and D. J. Fox, Gaussian, Inc., Wallingford CT, 2009.

[31] I. Felhosi, J. Telegdi, G. Palinkas and E. Kalman, “Kinetics of self-assembled layer formation on iron”, Electrochim. Acta, 47 (2002) 2335–2340.

[32] G. Gusmano, P. Labella, G. Montesperelli, A. Privitera and S. Tassinari, “Study of the Inhibition Mechanism of Imidazolines by Electrochemical Impedance Spectroscopy”, Corros., 62 (2006) 576–583.

[33] H. Ashassi-Sorkhabi and E. Asghari, “Effect of hydrodynamic conditions on the inhibition performance of l-methionine as a “green” inhibitor”, Electrochimica Acta, 54 (2008) 162–167.

[34] X. Li, S. Deng, H. Fu and G. Mu, "Synergistic inhibition effect of rare earth cerium (IV) ion and anionic surfactant on the corrosion of cold rolled steel in H_2SO_4 solution", Corros. Sci., 50 (2008) 2635–2645.

[35] P. Bommersbach, C. Dumont Alemany, J. P. Millet, B. Normand, “Formation and behaviour study of an environment-friendly corrosion inhibitor by electrochemical methods”, Electrochim. Acta, 51 (2005) 1076–1084.

[36] W. F.Wayne and G. H.Sonald, “Green inhibitors – development and applications for aqueous systems”, Corros., Schlumberger, Nace Int., Houston, 23 (2004) 4407–4418.

[37] J. Crousier, C. Antonione, Y. Massiani and J.P. Crousier Effect of chromium on the corrosion resistance of amorphous Fe-Ni-B-P alloys in 0.1 N H_2SO_4, Mat. Chem., 7 (1982) 587–604.

[38] S.T. Arab and K. M. Emran, “Thermodynamic study on Corrosion Inhibition of Fe78B13Si9 Metallic Glass Alloy in Na_2SO_4 Solution at Different Temperatures” Int. J. App., Chem., 3 (2007) 69–84.

[39] T. Szauer and A. Brand “Adsorption of oleates of various amines on iron in acidic solution”, Electrochem. Acta., 26 (1981) 1253–1256.

[40] S. Sankarapapavinasam, F. Pushpanaden and M. Ahmed, “Piperidine, piperidones and tetrahydrothiopy"rones as inhibitors for the corrosion of copper in H_2SO_4”, Corros. Sci., 32 (1991) 193–203.

[41] T. P. Hoar and R. D. Holliday, “The inhibition by quinolines and thioureas of the acid dissolution of mild steel”, J. Appl. Chem., 3 (1953) 502–513.

[42] Obi-Egbedi, N.O. Obot and I.B. Obot “Xanthione: A new and effective corrosion inhibitor for mild steel in sulphuric acid solution” Arabian J. of Chemistry 6 (2013)211–223

[43] A. Y. Musa, A. H. Kadhum and A. Mohamad, “A comparative study of the corrosion inhibition of mild steel in sulphuric acid by 4,4-dimethyloxazolidine-2-thione”, Corros. Science. 51 (2009) 2393–2399.

[44] L. Larabi, O. Benali, S. M. Mekelleche and Y. Harek, “2-Mercapto-1-methylimidazole as corrosion inhibitor for copper in hydrochloric acid”, Applied Surface Science, 253(2006)1371–1378.

[45] M. K. Awad , M. S. Metwally , S.A. Soliman , A.A. El-Zomrawy and M.A. bedair,"Experimental and quantum chemical studies of the effect of poly ethylene glycol as corrosion inhibitors of aluminum surface", J. of Industrial and Engineering Chemistry 20 (2014) 796–808.

[46] G. K. Gomma and M. H. Wahdan “Schiff bases as corrosion inhibitors for aluminium in hydrochloric acid solution”, Materials Chemistry and Physics, 39 (1995) 209–213.

[47] N. Soltani, M. Behpour , S.M. Ghoreishi and H. Naeimi, “Corrosion inhibition of mild steel in hydrochloric acid solution by some double Schiff bases”, Corros. Science, 52 (2010) 1351–1361.

[48] M. Behpour, S.M. Ghoreishi, M. Khayatkashani and N. Soltani “The effect of two oleo-gum resin exudate from Ferula assa-foeita and Dorema ammoniacum on mild steel corrosion in acidic media”,

Corros. Science, 53(2011) 2489–2501.
[49] K. Tebbji, N. Faska , A. Tounsi A., H. Oudda and M. Benkaddour "The effect of some lactones as inhibitors for the corrosion of mild steel in 1M hydrochloric acid", Materials Chemistry and Physics,106 (2007) 260–267.
[50] E. Kamis, F. Belluscci, R. M. Latanision and E. S. H. El-Ashry "Acid Corrosion Inhibition of Nickel by 2-(Triphenosphoranylidene) Succinic Anhydride,", Corros., 47 (1991) 677–686.
[51] F. Donahue and K. Nobe, "Theory of Organic Corrosion Inhibitors: Adsorption and Linear Free Energy Relationships", J. Electrochem. Soc., 112 (1965) 886–890.
[52] W. Durnie, R.D. Marco, A. Jefferson and B. Kinsella "Development of a Structure-Activity Relationship for Oil Field Corrosion Inhibitors", J. Electrochem. Soc., 146 (1999) 1751–1756.
[53] O. Benali, L. Larabi, M. Traisnel , L. Gengenbre, Y. Harek, "Electrochemical, theoretical and XPS studies of 2-mercapto-1-methylimidazole adsorption on carbon steel in 1 M HClO4", Appl. Surf. Sci., 253 (2007) 6130–6139.
[54] G. Quartarone, M. Battilana, L. Bonaldo and T. Tortato, "Investigation of the inhibition effect of indole-3-carboxylic acid on the copper corrosion in 0.5 M H2SO4", Corros. Sci. 50 (2008) 3467–3474.
[55] M. A. Hegazy, H. M. Ahmed and A. S. El-Tabei "Investigation of the inhibitive effect of p-substituted 4-(N, N, N-dimethyldodecylammonium bromide) benzylidene-benzene-2-yl-amine on corrosion of carbon steel pipelines in acidic medium", Corros. Sci. 53 (2011) 671–678.
[56] L. Finar, 6th ed., Organic Chemistry, vol. 1, Longman, London, 1986.
[57] M. Guan-Nan, L. Xiang-Hong, Q. Qing and Z. Jun "Synergistic Effect on Corrosion Inhibition by Cerium (IV) Ion and Sodium Molybdate for Cold Rolled Steel in Hydrochloric Acid Solution", Acta Chim. Sin. 62 (2004) 2386–2390
[58] M. Ozcan, I. Dehri, M. Erbil, Applied Surface Science. 236 (2004) 155–164.
[59] A.S. Fouda, A.S. Ellithy, Corrosion Science., 51 (2009) 868–875
[60] K.F. Khaled, M.M. Al-Qahtani, Materials Chemistry and Physics., 113 (2009) 150–158
[61] H.F. Finley, N. Hackerman, J. Electrochem. Soc., 107 (1960) 259.
[62] N. Khalil, Electrochim. Acta ., 48 (2003) 2635.
[63] G. Bereket, E. Hur, C. Ogretir, J. Mol. Struct. (Theochem)., 578 (2002) 79.
[64] A. K Mohamed, T. H. Raha , N. N. H. Moussa, Bull Soc. Chim Fr., 127 (1990) 375.
[65] O. Benali, L. Larabi, S.M. Mekelleche, Y. Harek, J. Mater. Sci., 41 (2006) 7064–7073.
[66] O. Benali, L. Larabi, M. Traisnel , L. Gengenbre, Y. Harek, Appl. Surf. Sci., 253 (2007) 6130.
[67] M. A. Amin, K. F. Khaled, Q. Mohsen H.A. Arida, Corrosion Science. 52 (2010) 1684–1695
[68] A. M. Al-Sabagh, N. M. Nasser, A. A. Farag, M. A. Migahed and A. M.F. Eissa, T. Mahmoud," Structure effect of some amine derivatives on corrosion inhibition efficiency for carbon steel in acidic media using electrochemical and Quantum Theory Methods,"Egyptian Journal of Petroleum, 22 (2013) 101–116.
[69] E. E. Ebenso, T. Arslan, K. Kandem, I. Love, C. Retlr, M.S. Lu and S.A. Umoren," Theoretical studies of some sulphonamides as corrosion inhibitors for mild steel in acidic medium", Int. Jour. Of Quantum Chem., 110 (2010) 2614-2636.
[70] I. Lukovits, E. Kalman, and F. Zucchi, "Corrosion inhibitors—correlation between electronic structure and efficiency", Corros., 57 (2001) 3–8.
[71] S. Martinez," Inhibitory mechanism of mimosa tannin using molecular modeling and substitutional adsorption sotherms", Materials Chem and Phy., 77 (2003) 97-102.
[72] J. C. Slater (Editor), Introduction to Chem and Physics, Dover, New York, (1970).
[73] E. E. Ebenso, M. M. Kabanda, T. Arslan, M. Saracoglu, F. Kandemirli, L. C. Murulana, A. K. Singh, S. K. Shukla, B. Hammouti, K.F. Khaled, M.A. Quraishi, I.B. Obot and N.O. Eddy," Quantum Chemical Investigations on Quinoline Derivatives as Effective Corrosion Inhibitors for Mild Steel in Acidic Medium ", Int. Jour. Electrochem. Sci., 7 (2012) 5643-5676.
[74] E. E. Ebenso, T. Arslan, F. Kandemirli, N. Caner and I. Love." Quantum chemical studies of some rhodanine azosulpha drugs as corrosion inhibitors for mild steel in acidic medium", Int. Jour. Quant. Chem., 10 (2010) 1003-1018.
[75] L. Larabi, O. Benali, S.M. Mekelleche, Y. Harek, Appl. Surf. Sci. 253, 1371 (2006)
[76] O. Benali, L. Larabi, M. Traisnel, L. Gengenbre, Y. Harek, Appl. Surf. Sci. 253, 6130 (2007)